

Supporting Information

Nano-engineering of a 3D-ordered membrane electrode assembly with ultrathin Pt skin on open-walled PdCo nanotube arrays for fuel cells

Yachao Zeng,^{a, b, †} Hongjie Zhang,^{a, b, †} Zhiqiang Wang,^{a, b} Jia Jia,^{a, b} Shu Miao,^c Wei Song,^a
Hongmei Yu,^{a,*} Zhigang Shao,^{a,**} Baolian Yi^a

*a. Fuel Cell System and Engineering Laboratory, Dalian Institute of Chemical Physics,
Chinese Academy of Sciences, Dalian, Liaoning 116023, China.*

b. University of Chinese Academy of Sciences, Beijing 100049, China.

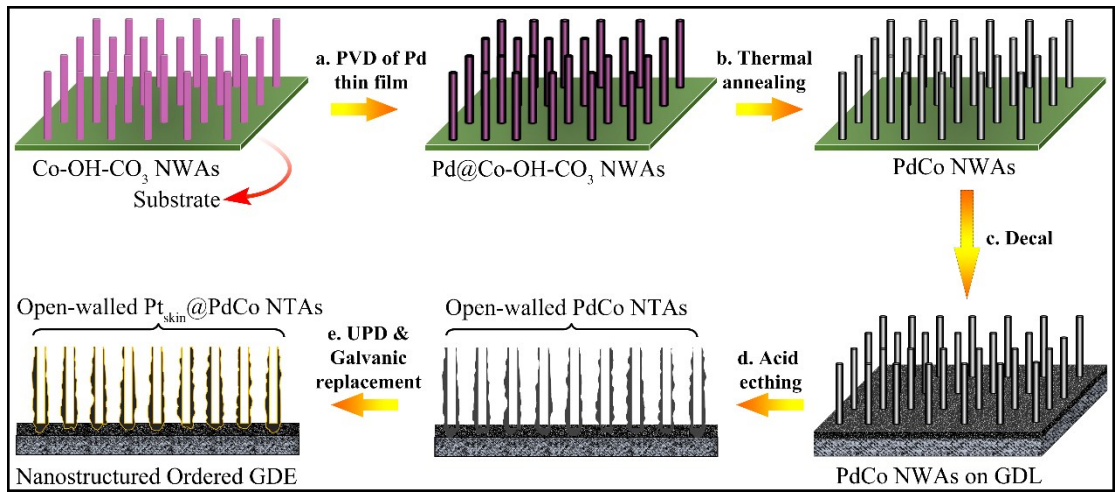
*c. Advanced Electron Microscopy Research Group, Dalian Institute of Chemical Physics,
Chinese Academy of Sciences, Dalian, Liaoning 116023, China.*

†. The authors contributed equally and can been considered as co-first authors.

**Corresponding Authors:*

Email: hmyu@dicp.ac.cn, zhgshao@dicp.ac.cn.

Fax: +86-84379518; Tel: +86-84379153.



Scheme S1. Schematic illustration of the fabrication process of the 3D-ordered GDE based on open walled Pt_{skin}@PdCo NTAs.

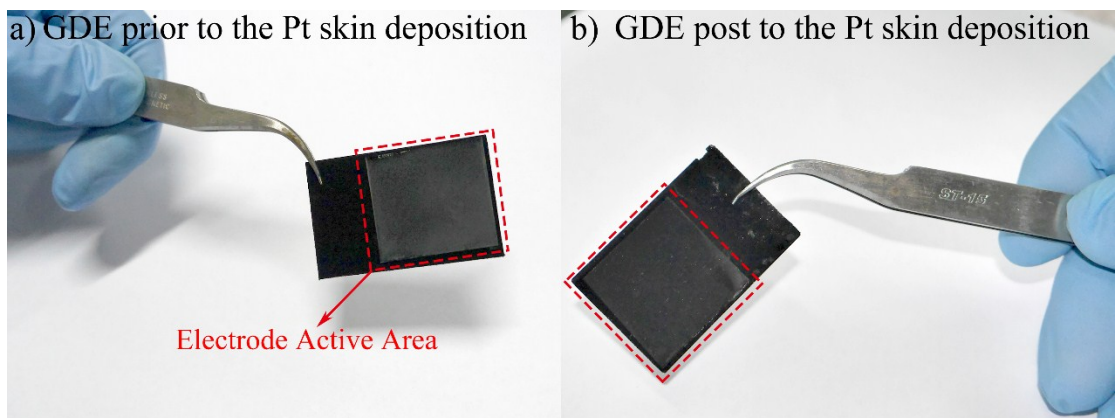


Figure S1. Optical images of the nanostructured GDEs based on PdCo NTAs-400 a) prior to and b) post to the Pt skin deposition.

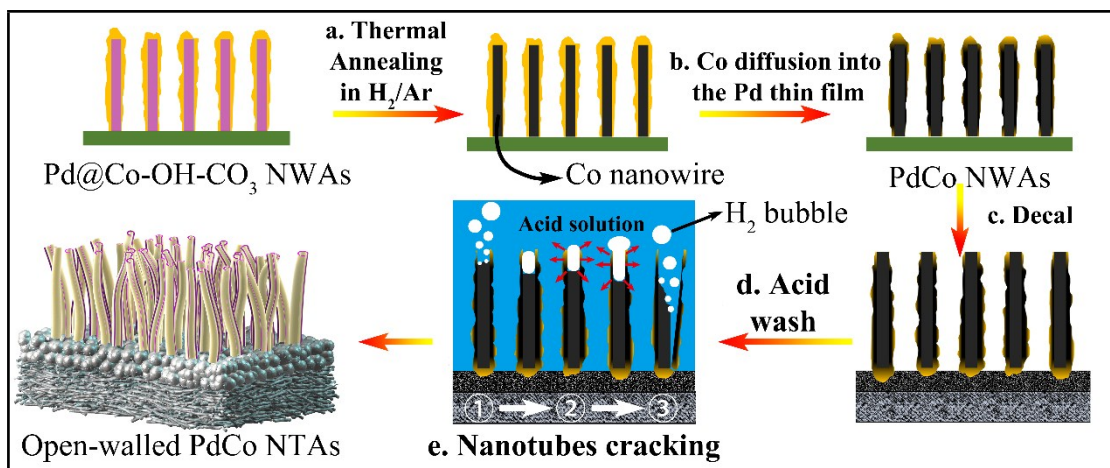


Figure S2. A schematic illustration of the formation process of the open-walled PdCo NTAs.

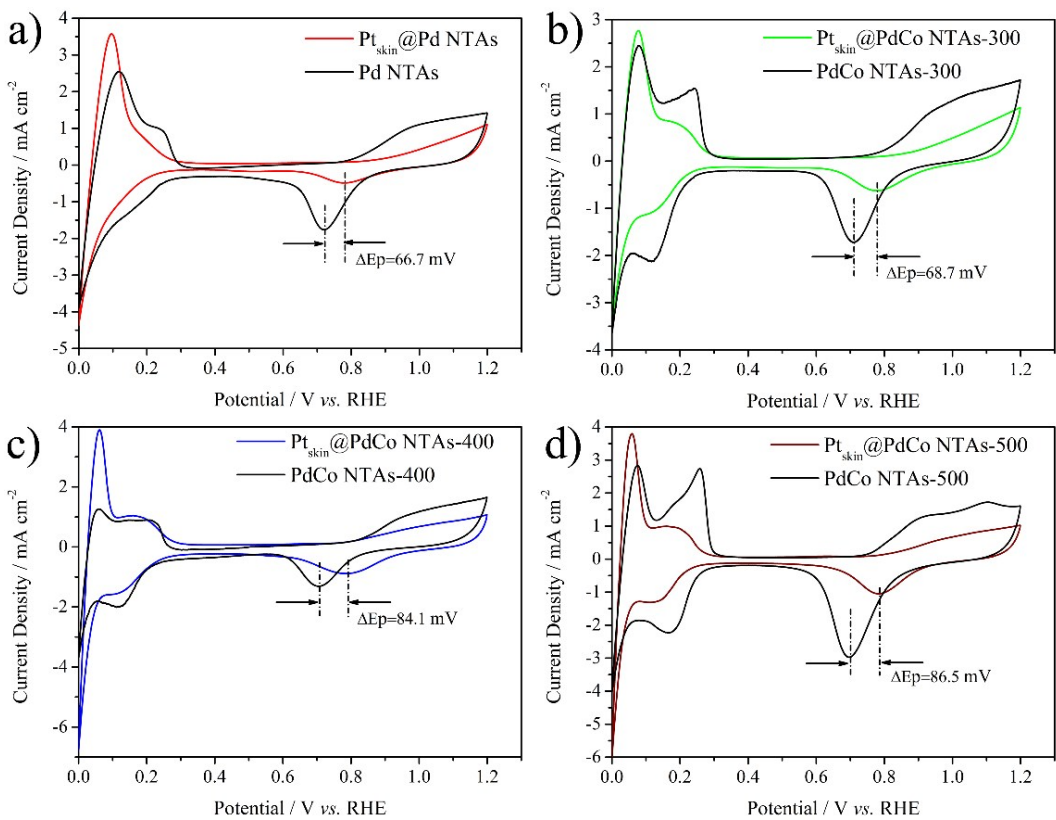


Figure S 3. Cyclic voltammograms of a) Pd NTAs-based, b) PdCo NTAs-300-based, c) PdCo NTAs-400-based and d) PdCo NTAs-500-based GDEs prior and post to the UPD and Galvanic displacement of Cu ML with Pt.

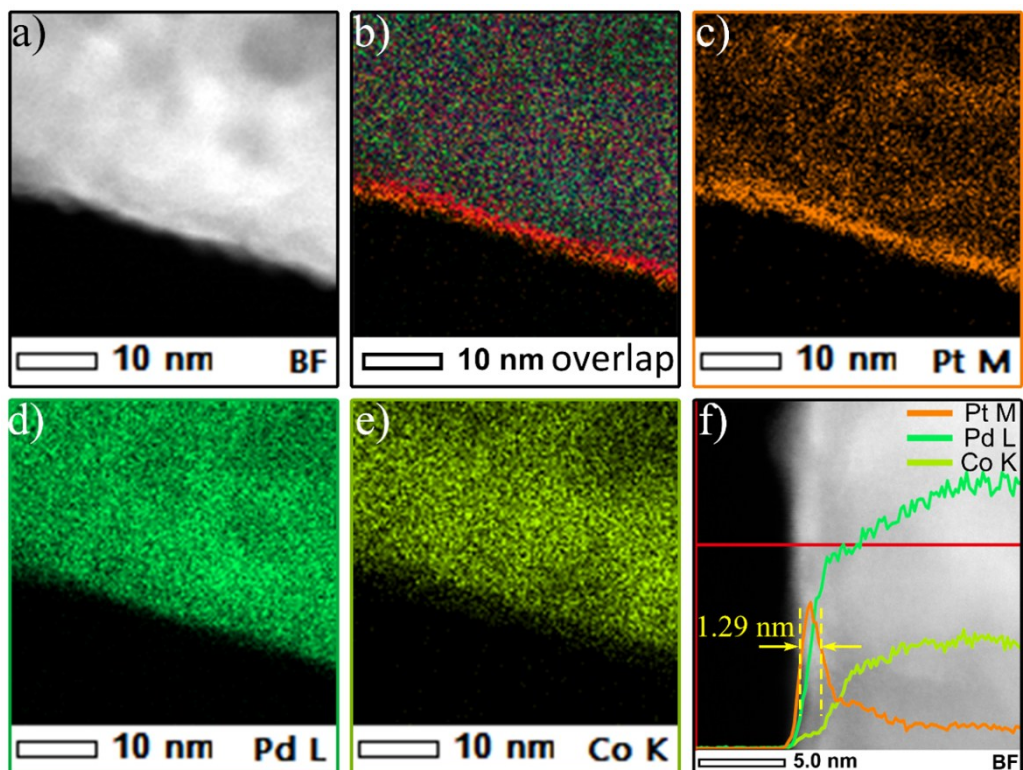


Figure S 4. a) ACSTEM image of $\text{Pt}_{\text{skin}}@\text{PdCo NTAs-400}$ and EDS elemental maps of c) Pt, d) Pd and e) Co. b) EDS map overlapping of Pt, Pd and Co. f) Distribution of elements in a $\text{Pt}_{\text{skin}}@\text{PdCo NTAs-400}$ obtained by a linear scan analysis EDS.

Table S1. A summary of crystal parameters derived from (220) panel of the prepared GDEs.

GDEs	2θ@(220) / degree	d-spacing / Å	Lattice parameters / Å
Pt/C (40 wt. %, JM)	67.60	1.38814	3.926
Pt _{skin} @Pd NTAs	67.61	1.38451	3.916
Pt _{skin} @PdCo NTAs-300	68.32	1.37179	3.880
Pt _{skin} @PdCo NTAs-400	68.79	1.36359	3.857
Pt _{skin} @PdCo NTAs-500	68.84	1.3669	3.866

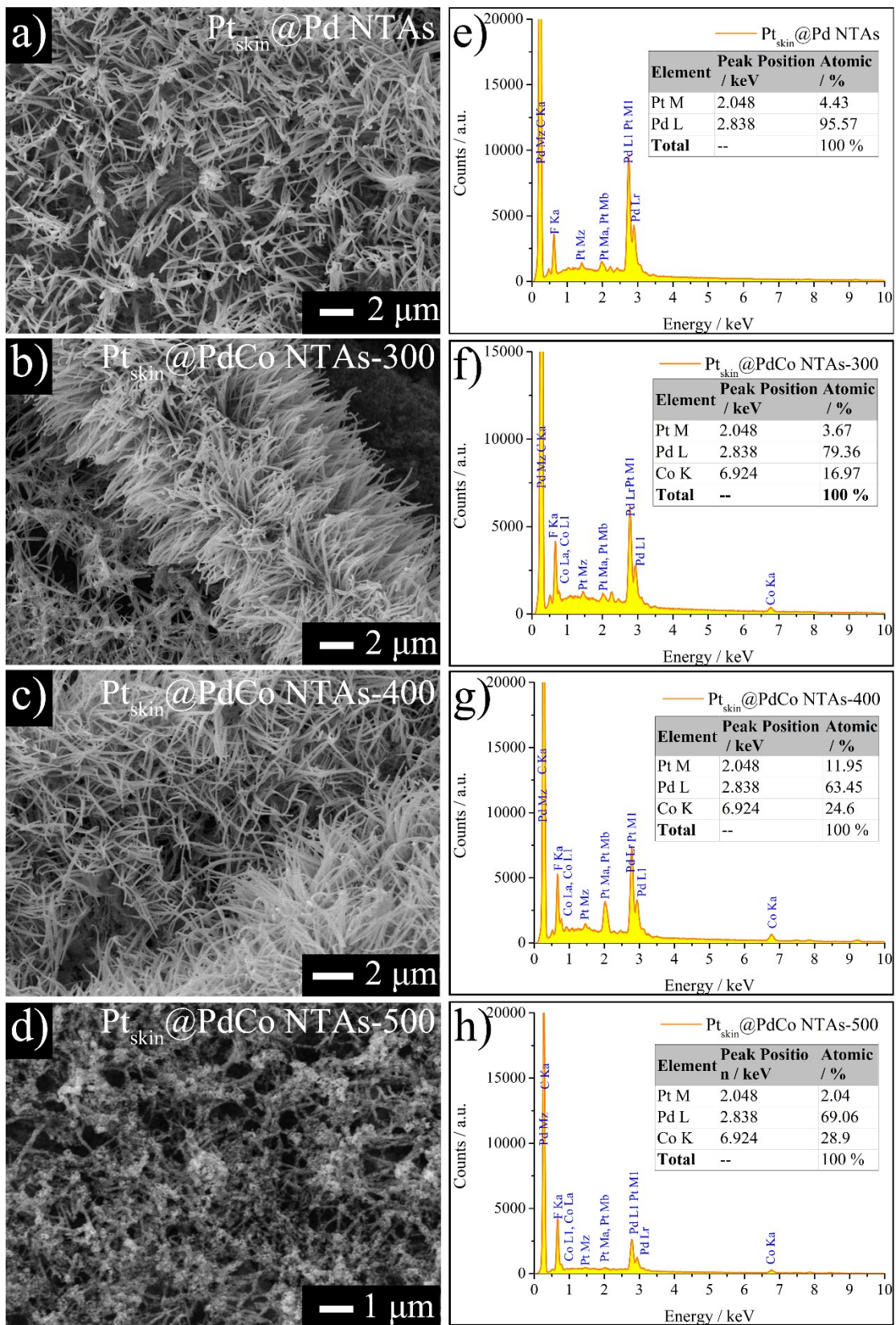


Figure S5. a-d) The in panel SEM images of the prepared nanostructured GDEs. e-h) The corresponding EDS spectra of the nanostructured GDEs.

Table S2. The atomic ratio of Pd : Co in Pd-based NTAs induced from thermal annealing.

GDEs	Atomic ratio of Pd to Co
Pt _{skin} @Pd NTAs	-
Pt _{skin} @PdCo NTAs-300	4.7:1
Pt _{skin} @PdCo NTAs-400	2.6:1
Pt _{skin} @PdCo NTAs-500	2.4:1

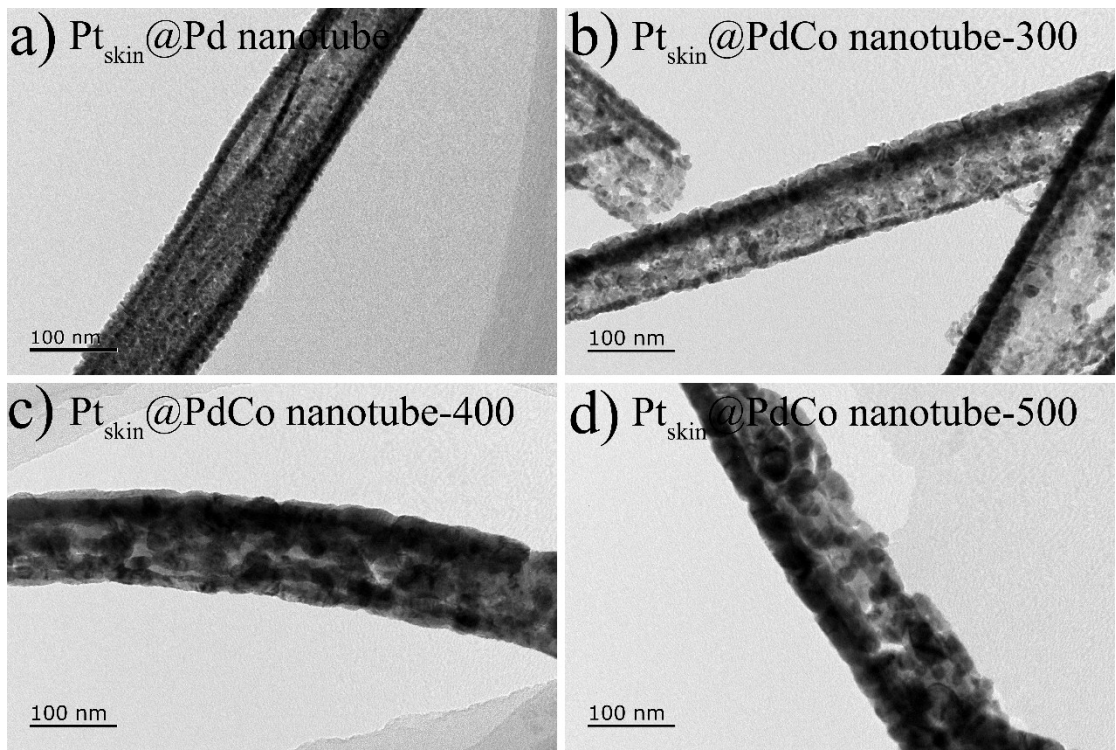


Figure S6. TEM images of a) $\text{Pt}_{\text{skin}}@\text{Pd}$ nanotube, b) $\text{Pt}_{\text{skin}}@\text{PdCo}$ nanotube-300, c) $\text{Pt}_{\text{skin}}@\text{PdCo}$ nanotube-400 and d) $\text{Pt}_{\text{skin}}@\text{PdCo}$ nanotube-500.

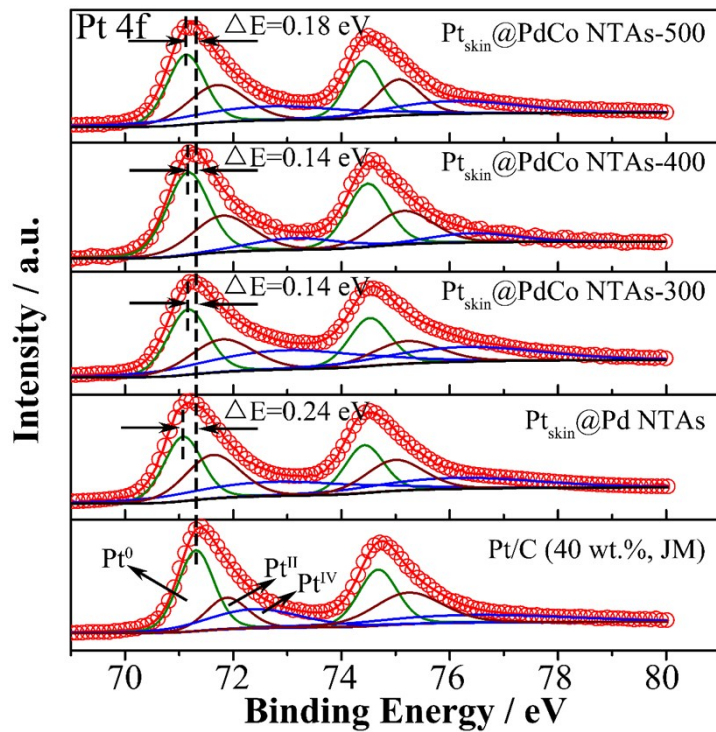


Figure S7. Pt 4f XPS spectra of the nanostructured GDEs and conventional GDE.

Table S 3. The Pt4f XPS data of the conventional and nanostructured GDEs.

Pt/C (40 wt.%, JM)		Pt _{skin} @Pd NTAs		Pt _{skin} @PdCo NTAs-300		Pt _{skin} @PdCo NTAs-400		Pt _{skin} @PdCo NTAs-500		
B. E. / eV	Ratio / %	B. E. / eV	Ratio / %	B. E. / eV	Ratio / %	B. E. / eV	Ratio / %	B. E. / eV	Ratio / %	
Pt ⁰	71.31	48.29	71.07	33.84	71.17	34.14	71.17	51.70	71.13	37.64
Pt ^{II}	71.89	21.96	71.63	32.88	71.80	26.62	71.81	32.29	71.71	30.63
Pt ^{IV}	72.38	29.76	72.78	33.28	72.96	39.25	73.15	16.01	72.7	31.74

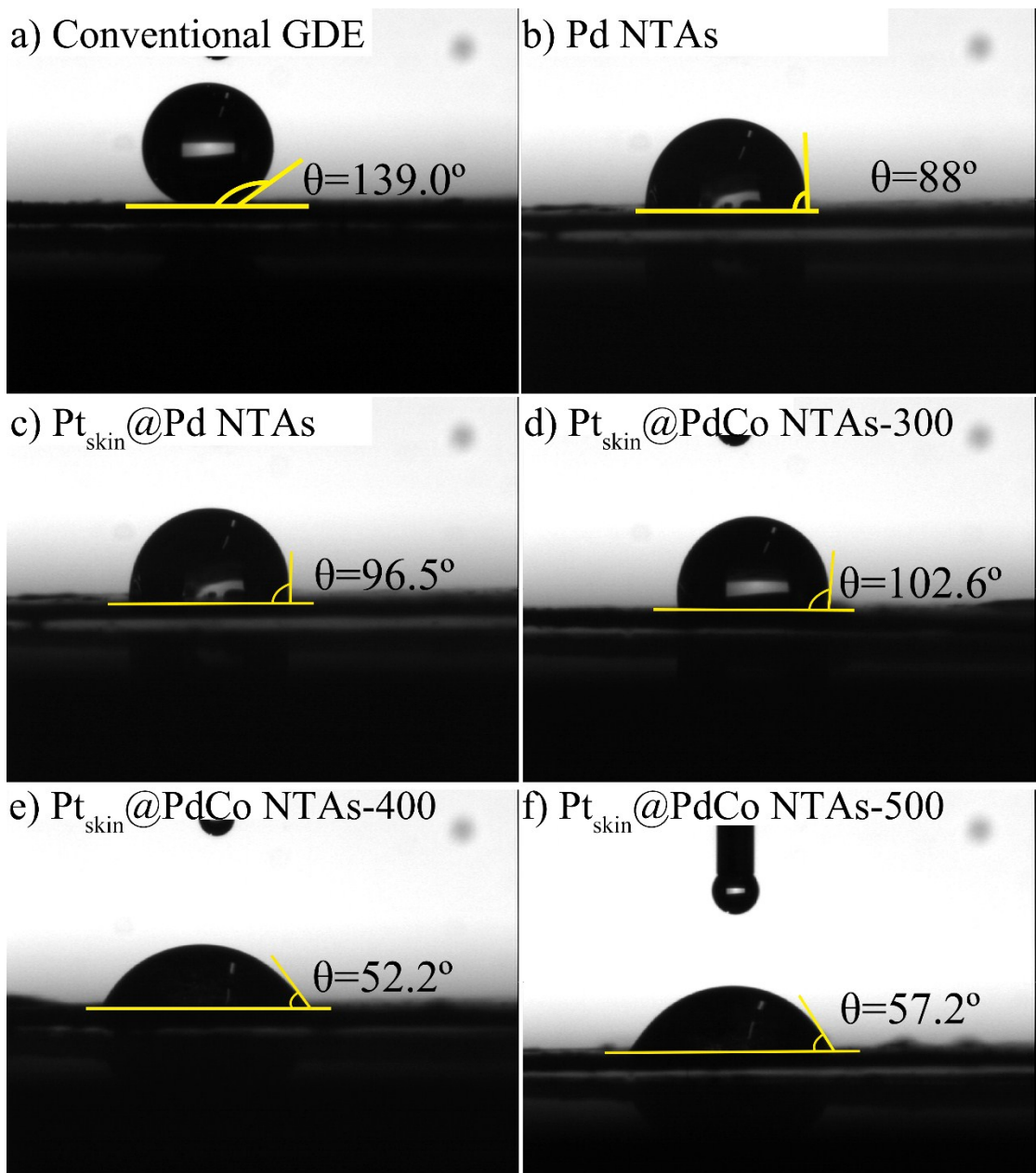


Figure S8. Contact angles of a) conventional Pt/C, b) Pd NTAs, c) $\text{Pt}_{\text{skin}}@\text{Pd NTAs}$, d) $\text{Pt}_{\text{skin}}@\text{PdCo NTAs-300}$, e) $\text{Pt}_{\text{skin}}@\text{PdCo NTAs-400}$ and f) $\text{Pt}_{\text{skin}}@\text{PdCo NTAs-500}$ based GDEs.

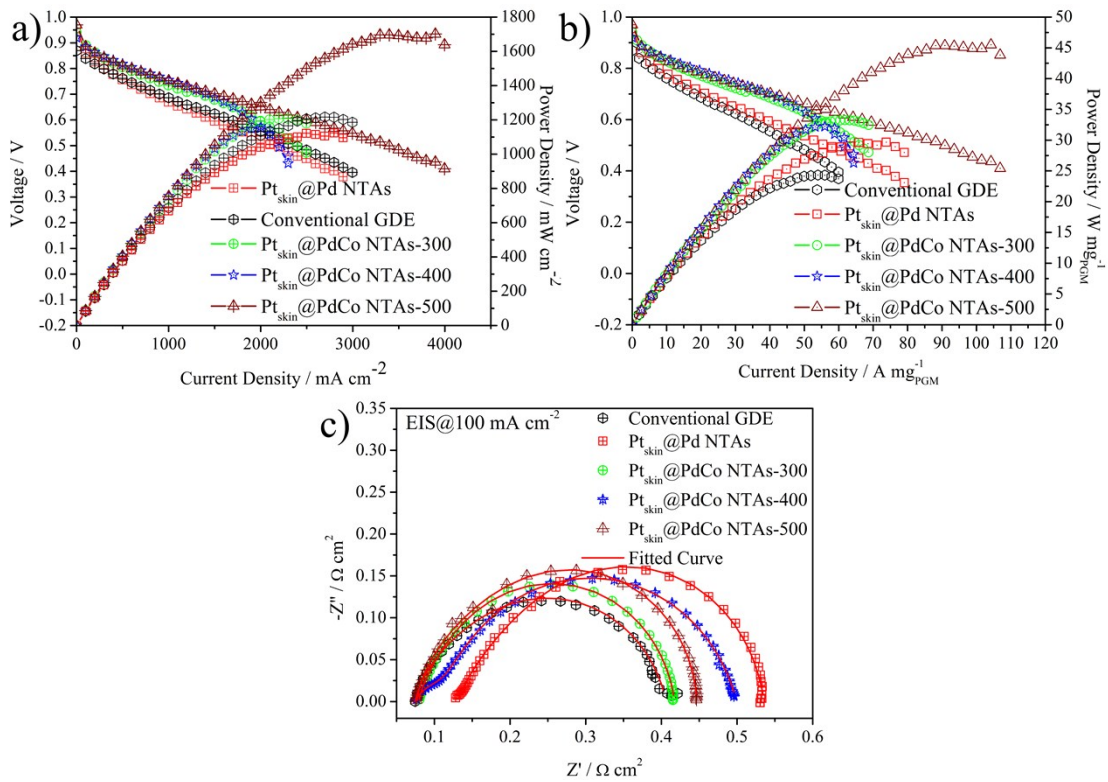


Figure S9. a) Electrode geometric specific and b) mass specific performances of the GDEs based on Pt/C, $\text{Pt}_{\text{skin}}@\text{Pd NTAs}$, $\text{Pt}_{\text{skin}}@\text{PdCo NTAs-300}$, $\text{Pt}_{\text{skin}}@\text{PdCo NTAs-400}$ and $\text{Pt}_{\text{skin}}@\text{PdCo NTAs-500}$ serving as anodes, testing conditions: active area: 2.56 cm^2 , 80°C , gas flow rate of H_2/O_2 was $100/200 \text{ mL min}^{-1}$, the gas humidity was 80 %. c) EIS recorded at a current density of 100 mA cm^{-2} .

Table S4. A summary of characteristic parameters of single cell performance with the prepared GDEs serving as anode.

Anodes	Power Density				
	mW cm^{-2}	$\text{kW g}_{\text{Pt}}^{-1}$	$\text{kW g}_{\text{PGM}}^{-1}$	$R_o / \text{m}\Omega \text{ cm}^2$	$R_{ct} / \text{m}\Omega \text{ cm}^2$
Conventional GDE	1218.7	24.4	24.4	59.9	82.8
$\text{Pt}_{\text{skin}}@\text{Pd NTAs}$	1122.0	198.9	29.6	129.7	128.5
$\text{Pt}_{\text{skin}}@\text{PdCo NTAs-300}$	1210.0	295.1	33.3	75.8	48.6
$\text{Pt}_{\text{skin}}@\text{PdCo NTAs-400}$	1151.6	323.0	32.2	76.4	29.3
$\text{Pt}_{\text{skin}}@\text{PdCo NTAs-500}$	1698.1	330.4	45.4	75.5	98.8

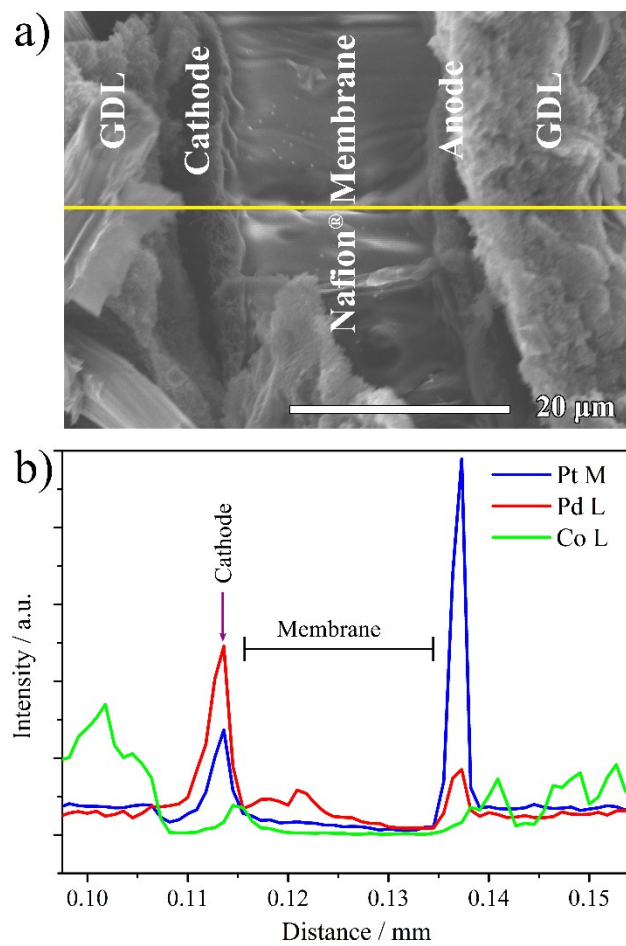


Figure S10. a) Cross sectional image of the $\text{Pt}_{\text{skin}}@\text{PdCo NTAs-400}$ -based MEA after 5000 ADT cycles, in which the yellow line labels the EDS analysis line. b) Elemental distributions in the aged $\text{Pt}_{\text{skin}}@\text{PdCo NTAs-400}$ -based MEA.